

Design of a Portable Low-Cost Impedance Analyzer

Abdulwadood Al-Ali¹, Ahmad Elwakil², Abdelaziz Ahmad² and Brent Maundy¹

¹*Dept. Elect. Computer Eng., University of Calgary, Calgary, Canada*

²*Dept. Elect. Computer Eng., University of Sharjah, Sharjah, U.A.E.*

Keywords: Bio-Impedance, Impedance Spectroscopy, Impedance Analyzer.

Abstract: Impedance analyzers available in the market are mostly bulky and often very expensive. In this paper, a low-cost, portable impedance analyzer is designed and implemented. The design utilizes the well-known, impedance network analyzer chip AD5933 and is capable of measuring a spectrum of impedances in the range 5 Hz to 100 kHz from 10 Ω to 100 k Ω . Its specifications allow it to be used in agriculture for monitoring the bio-impedance of fruits in different stages of their lives, especially during the growth period while maintaining low-cost.

1 INTRODUCTION

Impedance spectroscopy is the study of the small-signal electrical response of an object to yield useful information about its structure “from mass transport, rates of chemical reactions, corrosion, and dielectric properties, to defects, microstructure, and compositional influences on the conductance of solids” (Barsoukov and Macdonald, 2005). Any property that affects the flow of current in a certain material can be investigated and studied through impedance spectroscopy (Barsoukov and Macdonald, 2005). Impedance spectroscopy has also been used extensively to investigate the behavior of biological tissues. Particularly monitoring the vitality of a fruit through different stages of its life (Rose et al., 2013) (Jamaludin et al., 2015). By measuring the impedance spectrum of a fruit, important properties can be correlated to this impedance such as the acidity and sugar content (Borges et al., 2012; Väinölä and Repo, 2000). The frequency range 10 Hz to 100 kHz, is satisfactory for most fruits. In that range, most fruits have an impedance magnitude between 10 Ω to 100 k Ω .

Few methods were previously discussed to extract the Cole-Cole impedance module (Cole and Cole, 1941), such as those in (Freeborn et al., 2013), (Maundy et al., 2015) and (Valente and Demosthenous, 2016). Meanwhile, there are hardly any portable low-cost impedance analyzers in the market that can be employed on a wide scale. Recall that agricultural applications cover large areas of land

hence the need for a battery operated low-cost wireless device.

In this work, we use the commercial AD5933 impedance analyzer chip along with an Atmel ATmega328P micro-controller unit (MCU) to achieve this task. The MCU sets the sweeping parameters in the AD5933 registers (the excitation voltage, the start frequency, the frequency increment and the number of steps) while managing the measured impedance data to be stored on a MicroSD card before being sent through Bluetooth to a PC for further processing. Many recently proposed impedance analyzer designs (Hoja and Lentka, 2013; Breniuc et al., 2014; Simic, 2013; Chabowski et al., 2015) have also employed the AD5933 since it is the only single chip impedance analyzer available in the market. However, overcoming its internal design limitations is not straight forward, as shall be explained below.

2 SYSTEM DESIGN

The proposed system, whose complete picture is shown in Fig. 1 uses an ATmega328P to control the AD5933 through its I^2C interface. To achieve, portability the measured impedance data is saved into an SD card and sent afterwards through Bluetooth to a PC using an HC-05 Bluetooth module. This module was chosen since it is widely used and well known for it is flexibility in choosing the baud rate, compatibility, low cost and low power consumption. The system is also provided with two 3.7V batteries of 4400mAh

to achieve full portability.

2.1 AD5933 and Analog Front-End

The AD5933 chip uses a voltage-controlled oscillator as an excitation signal. It has a precise direct digital synthesizer (DDS) and impedance measurement is done by sensing the current going through the unknown impedance under test, converting it to a voltage and then using an internal 12-bit analog to digital converter (ADC) along with a Discrete Fourier Transform (DFT) engine to extract the real (R) and imaginary (I) parts of the impedance. The extracted R and I values are saved in the chip's registers which can be accessed through an I²C interface. However, the AD5933 has the following limitations:

2.1.1 Frequency Range

The AD5933 has the ability to do measurements within the frequency range 1 kHz to 100 kHz without any external components. The lower limit of this frequency range is affected by the ADC sampling rate which in turn defines the resolution of the DFT as shown by equations (1) and (2) (Devices, 2012)

$$ADC \text{ Sampling rate} = \frac{MCLK}{16} \quad (1)$$

$$DFT \text{ Resolution} = \frac{ADC \text{ Sampling rate}}{1024} \quad (2)$$

Using the internal on chip oscillator, the excitation frequency can't go below 1 kHz since it is provided with a 16.778 MHz clock that will therefore result in a 1.04 MHz sampling rate which will limit the DFT resolution to 1 kHz. For the excitation signal frequency to go below 1 kHz, the clock that drives the AD5933 has to be changed for each range of frequencies. The authors of (Chabowski et al., 2015) showed that the excitation signal frequency (f_w) can be chosen precisely and that the spectral leakage and the spikes in the current to voltage converter can be avoided by using equation (3) with integer values of k between 16 and 32 (Devices, 2012).

$$f_w = k \cdot \frac{MCLK}{1024 \times 16} \quad (3)$$

Using this equation, we control the master clock ($MCLK$) using an external programmable oscillator which lowered the limit of the frequency to 5 Hz. However, the upper frequency limit cannot be changed since it was limited to 100 kHz by the anti-aliasing filter located before the ADC internal to the chip.

2.1.2 DC Cancellation

Although the AD5933 has a perfect DDS core that can provide very precise excitation signals at different frequencies, this excitation signal has a DC-bias which is different for each excitation amplitude. A DC voltage difference across biological cells under test might cause polarization (Chabowski et al., 2015). Therefore, a high pass filter is necessary to cancel the DC component of the excitation before reaching the unknown impedance. We employed a passive RC filter with a cutoff frequency of 135 mHz in our design, which was a sufficient solution for DC cancellation and it did not add any complexity to the design.

2.1.3 Output Impedance

The AD5933 has an output impedance that depends on the excitation amplitude and that can be relatively high in some cases (Devices, 2012; Devices, 2013a). To solve this problem, a buffer with a very low output impedance was added to isolate the unknown impedance from the chip (Devices, 2013c).

2.1.4 Impedance Range

The measurable impedance range is affected by the linearity and the calibration process inside the chip. The manufacturer circuit note recommends using a simple inverting amplifier with gain $-R_{fb}/Z_{unknown}$ in order to sense the current in the unknown impedance and convert it to voltage (Devices, 2013b). The ADC inside the chip is limited in terms of its input voltage to the range 15mV-5V (Chabowski et al., 2015). Since the input of the ADC (V_{ADC}) is given by

$$V_{ADC} = V_{in} \times -(R_{fb}/Z_{unknown}) \times PGA_{gain} \times FilterGain \quad (4)$$

and since the on-chip PGA and filter both have unity gain, the linearity of the ADC depends only on the ratio $R_{fb}/Z_{unknown}$. Our extensive experiments have shown that the linearity of the gain factor (used in the calibration process) can only be preserved by keeping the ratio $R_{fb}/Z_{unknown}$ between $\frac{1}{3.5}$ and 3.5. Therefore, to expand the measurable magnitude of $Z_{unknown}$, a multiple R_{fb} solution was adopted where four different values of R_{fb} (33 Ω , 330 Ω , 3.3 k Ω and 33 k Ω) were switched into the circuit through two (single pole, double throw) switches switch as needed (Devices, 2004).

2.2 Data Processing

The AD5933 needs to be calibrated with a known impedance by calculating the gain factor which repre-

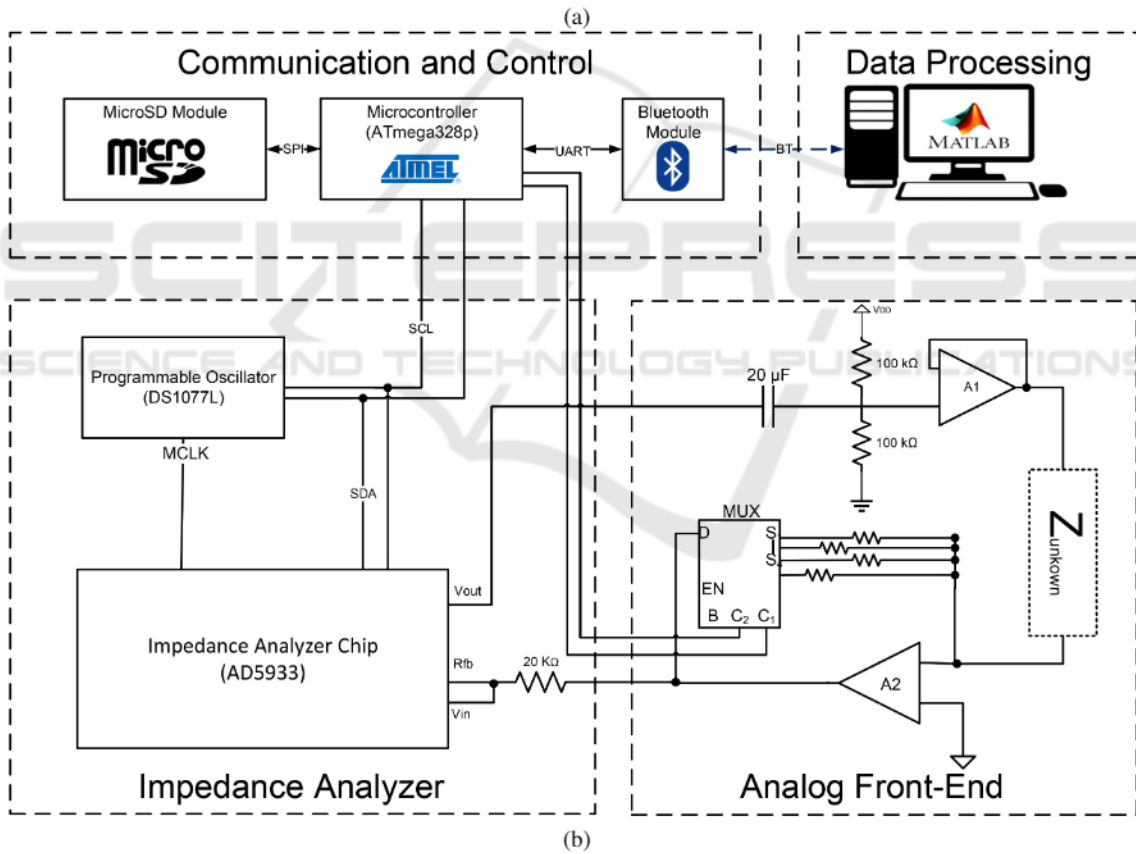
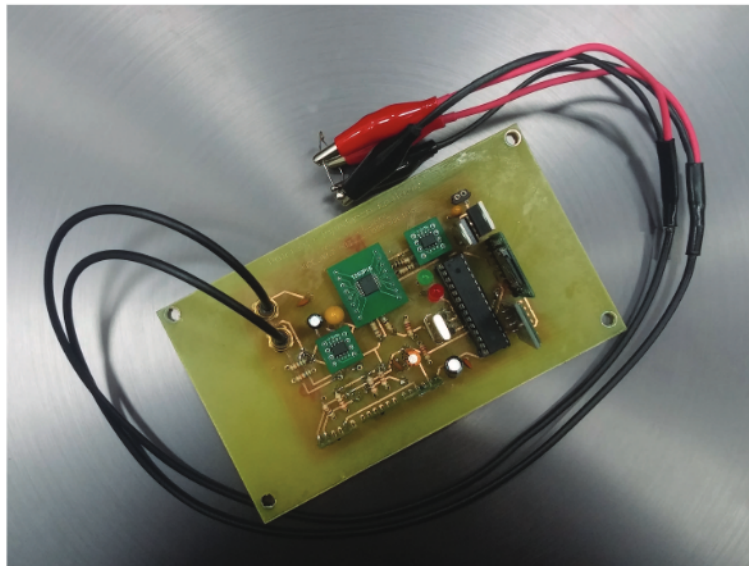


Figure 1: The designed portable impedance analyzer. (a) PCB implementation (b) System Design.

sents the gain of the system calculated using equation (5)

$$GainFactor = \frac{\left(\frac{1}{R_c}\right)}{\sqrt{R^2 + I^2}} \quad (5)$$

where R_c is the calibration resistor value while R and

I are the values in the real and imaginary registers respectively. The calibration methods mentioned in the AD5933 datasheet are typically for small frequency ranges. In the proposed design calibration is being done using a lookup table to provide a gain factor value for each point in the sweep which reduces the

error in the measurements significantly. After calculating the impedance magnitude, the phase should be also calibrated by using a resistor to get the system phase that should be subtracted from the calculated phase as

$$\text{Unknown Phase} = (\Phi_{\text{measured}} - \Phi_{\text{System}}) \quad (6)$$

where Φ_{System} is the phase of the system calculated using a known calibration resistor (where $\Phi = \tan^{-1}(\frac{I}{R})$).

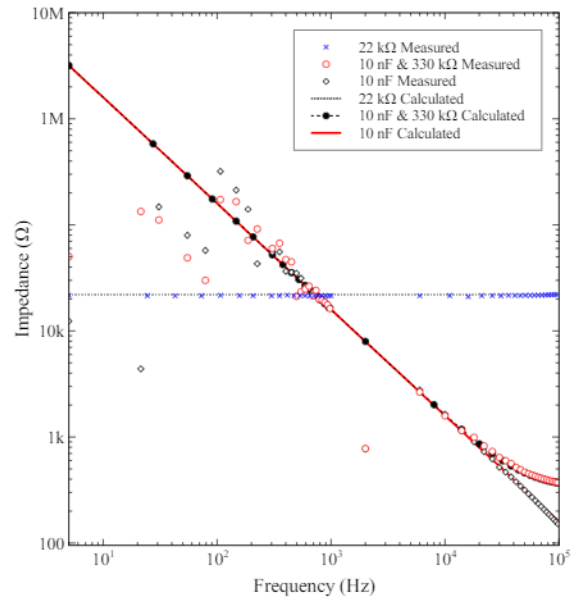
3 EXPERIMENTAL RESULTS

The device was first tested using off shelf resistive and capacitive components with standard tolerances. The measured magnitude and phase are shown respectively in Figs. 2(a) and (b) for the following cases: A 22 k Ω Resistor, 10 nF Capacitor and an RC combination of 330 Ω series with 10 nF. The theoretical values are also plotted in the same figure.

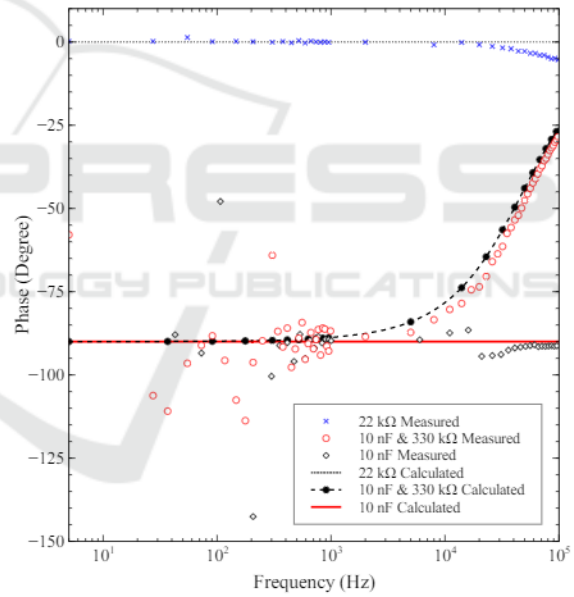
The impedance of two different apples was then measured using both our device and the industry standard PSM3750 impedance analyzer (Newton 4th LTD, UK) fitted with an IAI fixture (Impedance Analysis Interface) (4th LTD, 2005). The measurements were done using gold plated electrodes and using the same placing for both measurements to minimize the error caused by electrodes place and type (Freeborn et al., 2016). The bode plot for both the magnitude and the phase is shown in Fig. 3 while the Nyquist plot is shown in Fig. 4. It is clear that the device provides acceptable results in comparison with one of the best devices in the market albeit with portability and very low cost of around \$150. Using an optimization and curve fitting algorithm to the measured data using our device, a double dispersion Cole-Cole model was constructed as shown in Fig. 5 (where $s = j\omega$) with the values in Table 1, and the Nyquist plot from the model is shown also in Fig. 4. The device testing showed that it draws around 170 mA in the worst case and is able to work for around 24 hours with the provided 4400 mAh batteries.

Table 1: Fitting model values.

Component	Apple #1	Apple #2
R_{∞} (Ω)	2.1947 k	1.4432 k
R_1 (Ω)	90.992 k	24.229 k
R_2 (Ω)	25.2579 k	45.323 k
C_1 (F)	9.7962E-07	2.3946E-08
α_1	0.8078	0.7383
C_2 (F)	3.2705E-08	6.9596E-07
α_2	0.7138	0.96447



(a)



(b)

Figure 2: Impedance (a) magnitude and (b) phase measurements from off shelf discrete components compared to actual values.

4 CONCLUSION

A portable low cost impedance analyzer was designed and implemented. The device can be left in the field to do continuous measurements for around 24 hours and the data can be obtained wirelessly afterwards for a low cost of around 150\$. It can measure impedance between 10 Ω and 100 k Ω , in a frequency range from

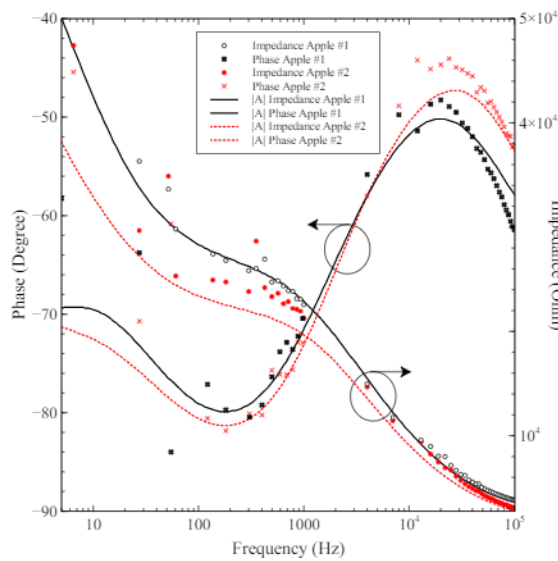


Figure 3: Comparison of measured phase and magnitude using the proposed device and the PSM3750-IAI results.

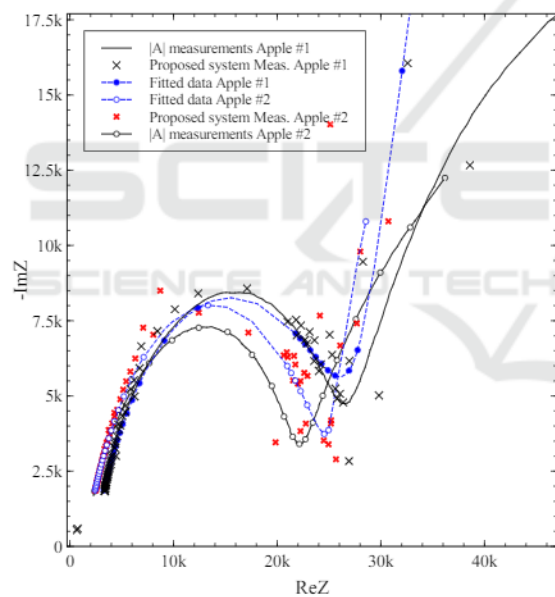


Figure 4: Impedance Nyquist plot measured using the proposed device compared to PSM3750-IAI measurements.

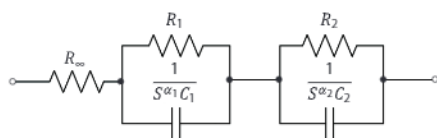


Figure 5: Double dispersion Cole-Cole fitting Model.

5 Hz to 100 kHz with a simple low-cost design. Such a device is very useful for studying a living object through different stages of its life without interrupting its natural behaviour. In agriculture the availabil-

ity of such an impedance analyzer makes it possible to determine a lot of information about the crops even before harvest, such as what practices contribute to the quality of the crops, the perfect time for harvest, determining the level of certain chemicals in the crops and many other factors.

REFERENCES

4th LTD, N. (2005). *IAI Impedance Analysis Interface user manual*.

Barsoukov, E. and Macdonald, J. (2005). *Impedance Spectroscopy: Theory, Experiment, and Applications*. John Wiley & Sons, 2 edition.

Borges, E., Matos, A., Cardoso, J., Correia, C., Vasconcelos, T., and Gomes, N. (2012). Early detection and monitoring of plant diseases by bioelectric impedance spectroscopy. In *Bioengineering (ENBENG), 2012 IEEE 2nd Portuguese Meeting in*, pages 1–4. IEEE.

Breniuc, L., David, V., and Haba, C.-G. (2014). Wearable impedance analyzer based on AD5933. In *Electrical and Power Engineering (EPE), 2014 International Conference and Exposition on*, pages 585–590.

Chabowski, K., Piasecki, T., Dzierka, A., and Nitsch, K. (2015). Simple wide frequency range impedance meter based on ad5933 integrated circuit. *Metrology and Measurement Systems*, 22(1):13–24.

Cole, K. S. and Cole, R. H. (1941). Dispersion and absorption in dielectrics i. alternating current characteristics. *The Journal of Chemical Physics*, 9(4):341–351.

Devices, A. (2004). *ADG849 3 V/5 V CMOS 0.5 SPDT/2:1 Mux in SC70 Data Sheet*.

Devices, A. (2012). *Evaluation Board User Guide UG-364*.

Devices, A. (2013a). *1 MSPS, 12-Bit Impedance Converter, Network Analyzer AD5933 Datasheet*. Rev. E.

Devices, A. (2013b). *AD5933 Circuit Note*. Rev. A.

Devices, A. (2013c). *AD8605/AD8606/AD8608 Datasheet*. Rev. N.

Freeborn, T. J., Elwakil, A. S., and Maundy, B. J. (2016). Electrode location impact on cole-impedance parameters using magnitude-only measurements. In *IEEE 59th Int. Midwest Symposium on Circuits and Systems (MWSCAS)*, volume 1, pages 21–24. IEEE.

Freeborn, T. J., Maundy, B., and Elwakil, A. S. (2013). Cole impedance extractions from the step-response of a current excited fruit sample. *Comput. Electron. Agric.*, 98:100–108.

Hoja, J. and Lentka, G. (2013). A family of new generation miniaturized impedance analyzers for technical object diagnostics. *Metrology and Measurement Systems*, 20(1).

Jamaludin, D., Aziz, S. A., Ahmad, D., and Jaafar, H. Z. (2015). Impedance analysis of labisia pumila plant water status. *Information Processing in Agriculture*, 2(3):161–168.

Maundy, B., Elwakil, A., and Allagui, A. (2015). Extracting the parameters of the single-dispersion cole

- bioimpedance model using a magnitude-only method. *Comput. Electron. Agric.*, 119(C):153–157.
- Rose, E. J., Pamela, D., and Rajasekaran, K. (2013). Apple vitality detection by impedance measurement. *International Journal of Advanced Research in Computer Science and Software Engineering*, 9:144–148.
- Simic, M. (2013). Realization of complex impedance measurement system based on the integrated circuit ad5933. In *Telecommunications Forum (TELFOR), 2013 21st*, pages 573–576.
- Väinölä, A. and Repo, T. (2000). Impedance spectroscopy in frost hardiness evaluation of rhododendron leaves. *Annals of Botany*, 86(4):799–805.
- Valente, V. and Demosthenous, A. (2016). Wideband fully-programmable dual-mode CMOS analogue front-end for electrical impedance spectroscopy. *Sensors*, 16(8):1159.

